Cognitive Neurodynamics (2022) 16:609–620
https://doi.org/10.1007/s11571-021-09741-7

RESEARCH ARTICLE

Assessing residual motor function in patients with disorders of consciousness by brain network properties of task-state EEG

Lipeng Zhang[1,2] · Rui Zhang[1,2,3] · Yongkun Guo[4] · Dexiao Zhao[4] · Shizheng Li[1,2] · Mingming Chen[1,2,3] · Li Shi[5,6] · Dezhong Yao[1,2,7] · Jinfeng Gao[1,2] · Xinjun Wang[4] · Yuxia Hu[1,2,3]

Received: 6 August 2021 / Revised: 27 September 2021 / Accepted: 24 October 2021 / Published online: 5 November 2021

Abstract

Recent achievements in evaluating the residual consciousness of patients with disorders of consciousness (DOCs) have demonstrated that spontaneous or evoked electroencephalography (EEG) could be used to improve consciousness state diagnostic classification. Recent studies showed that the EEG signal of the task-state could better characterize the conscious state and cognitive ability of the brain, but it has rarely been used in consciousness assessment. A cue-guide motor task experiment was designed, and task-state EEG were collected from 18 patients with unresponsive wakefulness syndrome (UWS), 29 patients in a minimally conscious state (MCS), and 19 healthy controls. To obtain the markers of residual motor function in patients with DOC, the event-related potential (ERP), scalp topography, and time–frequency maps were analyzed. Then the coherence (COH) and debiased weighted phase lag index (dwPLI) networks in the delta, theta, alpha, beta, and gamma bands were constructed, and the correlations of network properties and JFK Coma Recovery Scale-Revised (CRS-R) motor function scores were calculated. The results showed that there was an obvious readiness potential (RP) at the Cz position during the motor preparation process in the MCS group, but no RP was observed in the UWS group. Moreover, the node degree properties of the COH network in the theta and alpha bands and the global efficiency properties of the dwPLI network in the theta band were significantly greater in the MCS group compared to the UWS group. The above network properties and CRS-R motor function scores showed a strong linear correlation. These findings demonstrated that the brain network properties of task-state EEG could be markers of residual motor function of DOC patients.

Keywords Disorders of consciousness · Residual motor function · Readiness potential · Coma recovery scale-revised scores · Brain network

✉ Yuxia Hu
huyuxia@zzu.edu.cn

[1] School of Electrical Engineering, Zhengzhou University, Zhengzhou, China

[2] Henan Key Laboratory of Brain Science and Brain-Computer Interface Technology, Zhengzhou, China

[3] Institute of Neuroscience of Zhengzhou University, Zhengzhou, China

[4] The Fifth Affiliated Hospital of Zhengzhou University, Zhengzhou, China

[5] Department of Automation, Tsinghua University, Beijing, China

[6] Beijing National Research Center for Information Science and Technology, Beijing, China

[7] The Clinical Hospital of Chengdu Brain Science Institute, MOE Key Lab for Neuroinformation, University of Electronic Science and Technology of China, Chengdu, China

Introduction

Disorders of consciousness (DOCs), caused by severe brain injury or nervous system disease, are abnormal states of consciousness (Giacino et al. 2014; Schiff and Plum 2000). According to the current 'gold standard' behavioral score, the JFK Coma Recovery Scale-Revised (CRS-R) (Giacino et al. 2004), patients with DOC are subdivided into those with unresponsive wakefulness syndrome (UWS) (Laureys et al. 2010) and those in a minimally conscious state (MCS) (Giacino et al. 2002). Although the behavioral score evaluates the patient from multiple dimensions, including hearing, vision, movement, communication, and arousal, the assessment is still susceptible to the subjective feelings of the attending doctors, leading to a high rate of misdiagnosis (Schnakers et al. 2009). Hence, searching for objective biomarkers related to the state of consciousness is of great significance to the assessment of patients with DOC.

Recently, electroencephalography (EEG) and functional magnetic resonance imaging (fMRI) have been adopted in some studies to assess the residual awareness of DOC patients (Malagurski et al. 2019; Bai et al. 2017a, 2020). Although fMRI has excellent spatial resolution, its high cost and unsuitability for patients undergoing cranial repair have hindered its clinical application. EEG has been accepted by most DOC researchers because of its high time resolution, easy operation, and low price. The resting state (Naro et al. 2018, 2016; Stefan et al. 2018), sleep (Wislowska et al. 2017; Mouthon et al. 2016; Rossi Sebastiano et al. 2018), event-related potentials (ERPs) (Li et al. 2015; Risetti et al. 2013; Rohaut et al. 2015), and TMS (Ragazzoni et al. 2013; Bai et al. 2017b; Bodart et al. 2017) EEG of DOC patients have been widely studied to extract characteristics for consciousness state assessment. But the oscillations in these EEG were spontaneous or evoked and did not correspond to cognitive processes. Compared to these non-task-state EEG, the brain neural activity corresponding to specific tasks could better reflect the residual consciousness of DOC patients. However, as far as we know, there has been no research on the task-state EEG of DOC patients.

Controlling voluntary movements is an important function of the brain and plays an important role in the assessment of the state of consciousness. Usually, a readiness potential (RP) can be recorded at the electrodes on frontal and central area prior to action (Kornhuber and Deecke 1965; Shibasaki and Hallett 2006). Also, during motor processes, there are event-related synchronization (ERS) and event-related desynchronization (ERD) phenomena (Pfurtscheller et al. 1999), as well as changes in the brain function network (Wisniewski et al. 2016; Nguyen et al. 2014). Relevant studies showed that some patients with UWS could attempt to complete some motor tasks (Cruse et al. 2011; Pan et al. 2020; Gui et al. 2020), but it was difficult for attending doctors to observe behavioral responses. Fortunately, the corresponding neural activities in the cerebral cortex might be captured by EEG. Hence, searching for task-related neural markers based on EEG is of great significance for the assessment of DOC patients' motor function.

In this study, a cue-guide motor task experimental paradigm for DOC patients was designed, and the EEG data of recruited participants were recorded synchronously. To obtain the neural markers used for motor function assessment, the RP and scalp topography were plotted and the values of time–frequency during motor preparation were calculated. Then, the brain networks of coherence (COH) and debiased weighted phase lag index (dwPLI) were constructed. Finally, the correlations of network properties and CRS-R motor function scores were analyzed.

Materials and methods

Patients

Forty-seven hospitalized DOC patients (18 females, 49.6 ± 14.5 years old) and 19 healthy subjects (7 females, 45.5 ± 13.9 years old, control group) were recruited in this study. The demographics and clinical data of recruited patients are shown in Table 1. The EEG data were collected in the Fifth Affiliated Hospital of Zhengzhou University. Before each experiment, the residual consciousness of each patient was assessed with CRS-R (Giacino et al. 2004) by a skilled physician. To ensure the consistency of the evaluation results, all the patients were evaluated by the same physician. The patients were further divided into an MCS group (29 patients, 6 females, 48.1 ± 13.3 years old) and a UWS group (18 patients, 12 females, 52.1 ± 16.3 years old). None of the patients had aneurysm clips, pacemakers, other implanted devices, or other drugs that might influence the EEG data. Each patient's legal representative had signed an informed consent form. This study was approved by the ethics committee of the Fifth Affiliated Hospital of Zhengzhou University.

Experimental design

The experimental paradigm is shown in Fig. 1. The block consisted of the experiment guide and the motor task trials. There was a 10 s interval between these two parts. All the cues were presented with auditory information and the

Table 1 The demographics and clinical data of recruited DOC patients

Patients	Clinical diagnosis	Gender/age	Etiology	Days since injury	CRS-R sub-scores	CRS-R total scores
P1	MCS	F/56	Hemorrhage	76	2 3 3 0 0 2	10
P2	MCS	F/56	Anoxia	70	3 3 3 1 1 2	13
P3	MCS	M/35	Anoxia	188	1 2 2 1 0 2	8
P4	MCS	F/56	Hemorrhage	111	3 3 3 0 1 2	12
P5	MCS	F/71	Hemorrhage	57	1 3 3 1 0 2	10
P6	MCS	F/67	Hemorrhage	113	1 3 3 0 0 2	9
P7	MCS	M/66	Hemorrhage	77	2 3 3 1 0 1	10
P8	MCS	M/54	Hemorrhage	153	2 3 2 1 0 1	9
P9	MCS	M/38	Trauma	275	1 3 3 2 0 2	11
P10	MCS	M/44	Hemorrhage	124	1 3 3 1 0 1	9
P11	MCS	M/38	Trauma	75	2 3 5 1 0 2	13
P12	MCS	M/48	Hemorrhage	63	1 3 2 1 0 1	8
P13	MCS	M/31	Trauma	134	3 0 5 1 1 2	12
P14	MCS	M/33	Trauma	111	3 3 2 1 1 2	12
P15	MCS	M/48	Hemorrhage	80	1 3 2 1 0 1	8
P16	MCS	F/30	Anoxia	129	4 4 5 2 2 3	20
P17	MCS	M/48	Trauma	98	2 2 2 1 0 2	9
P18	MCS	M/33	Trauma	138	4 3 2 1 2 3	15
P19	MCS	M/48	Trauma	98	2 3 3 1 0 2	11
P20	MCS	M/31	Trauma	166	3 3 5 1 1 2	15
P21	MCS	M/64	Hemorrhage	108	3 4 3 2 1 3	16
P22	MCS	M/37	Anoxia	740	1 0 3 1 0 2	7
P23	MCS	M/38	Trauma	236	1 3 3 1 0 2	10
P24	MCS	M/64	Hemorrhage	108	3 4 3 2 1 3	16
P25	MCS	M/33	Trauma	180	4 3 2 1 2 3	15
P26	MCS	M/64	Trauma	32	1 3 3 1 0 2	10
P27	MCS	M/64	Hemorrhage	120	3 5 3 2 1 3	17
P28	MCS	M/38	Trauma	257	1 3 3 1 0 2	10
P29	MCS	M/62	Trauma	42	1 3 2 1 0 2	9
P30	UWS	F/49	Trauma	68	1 1 2 1 0 1	6
P31	UWS	F/74	Trauma	75	1 0 2 0 0 2	5
P32	UWS	F/31	Anoxia	61	1 0 2 0 0 2	5
P33	UWS	M/72	Anoxia	135	1 0 2 1 0 1	5
P34	UWS	M/65	Trauma	38	0 0 1 1 0 1	3
P35	UWS	M/37	Anoxia	730	1 0 2 1 0 2	6
P36	UWS	M/72	Anoxia	107	1 0 2 1 0 1	5
P37	UWS	F/45	Trauma	36	0 1 2 0 0 1	4
P38	UWS	F/31	Anoxia	77	1 0 2 0 0 2	5
P39	UWS	F/58	Hemorrhage	104	1 1 0 0 0 2	4
P40	UWS	F/58	Hemorrhage	120	1 1 2 0 0 2	6
P41	UWS	F/60	Trauma	330	1 0 2 1 0 2	6
P42	UWS	F/31	Anoxia	61	1 0 2 0 0 2	5
P43	UWS	M/65	Trauma	60	0 0 2 1 0 2	5
P44	UWS	F/64	Hemorrhage	91	0 0 2 1 0 1	4
P45	UWS	M/47	Trauma	70	0 0 2 0 0 1	3
P46	UWS	F/58	Hemorrhage	146	1 1 2 0 0 2	6

Table 1 (continued)

Patients	Clinical diagnosis	Gender/age	Etiology	Days since injury	CRS-R sub-scores	CRS-R total scores
P47	UWS	F/21	Anoxia	171	1 0 2 1 0 2	6

M male, *F* female. Six CRS-R sub-scores indicate the assessment of auditory, visual, motor, verbal, and communication functions, and arousal. None of the patients showed obvious behavioral responses during EEG data recording

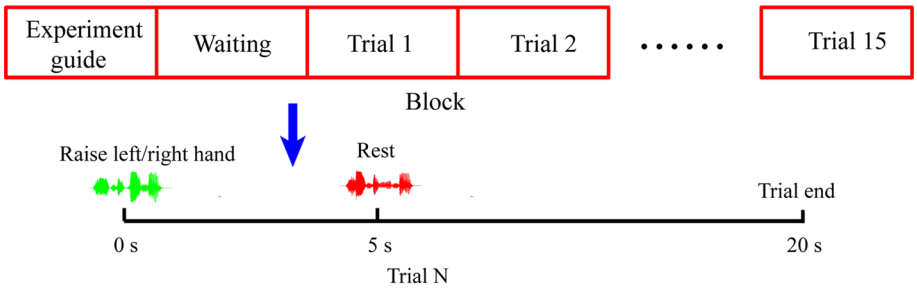

Fig. 1 Illustration of the cue-guide motor task experimental design

patients wore a headset during the experiment. In the experiment guide stage, the subjects were informed of the experiment tasks and precautions. In the motor task stage, 15 trials were played sequentially. At the beginning of each trial, the subject heard a voice say, 'raise your left hand,' or, 'raise your right hand' (the choice of left or right hand was based on the clinician's recommendation). Then, 5 s was allotted for the subject to perform the motor task. This was followed by a voice saying 'rest', and the subject had 15 s rest time. Each subject completed two blocks of the experiment, so 30 trials were completed by each subject. The subject's eyes keep open during the experiment.

Data recording and pre-processing

In the experiment, the data were collected with a 29-channel EEG recorder (Nicolet EEG V32, Natus, United States) and three expansion channels (two marker channels and one EMG channel). The following channels were selected: Fp1, Fp2, FC3, FC4, CP3, CP4, Fz, Cz, Pz, FCz, F3, F4, C3, C4, P3, P4, FT7, FT8, F7, F8, T3, T4, T5, T6, TP7, TP8, O1, O2, and Oz, and the channel positions were consistent with the International 10–20 system. The linked ears reference was used as the EEG data reference electrode. The signals were notch filtered at 50 Hz and the sampling rate was set to 1000 Hz. During the data recording process, the impedance of all electrodes was kept below 5 kΩ. The EMG were recorded for all subjects, but the patients did not produce effective limb movement, so the EMG data of all the patients were excluded.

To obtain motor onset time, the EMG data of the control group were analyzed. With a zero-phase shift bandpass filter, the EMG data were first filtered by cut-off frequencies of 6 and 50 Hz. Then, the energy of the filtered data was calculated, and the motor onset time was obtained by choosing a proper threshold (Hu et al. 2017).

EEG data preprocessing was performed using MATLAB and the EEGLAB toolbox (Delorme and Makeig 2004). First, EEG data were resampled to 500 Hz and filtered with a zero-phase shift bandpass filter at 0.1 to 45 Hz. Then, the bad data segments were removed manually, and bad channels were replaced with the average of nearby channels. Independent component analysis (ICA) was used to reject artifacts (EMG, EOG, and electrocardiogram) (Jung et al. 2000). By observing the temporal and spatial characteristics of the components, these components were removed manually. The preprocessed EEG were re-referenced to the reference electrode standardization technique (REST) (Yao 2001) and segmented to 10 s epochs (5 s before and after the audio cue). The amplitudes of epochs that exceeded [−100, 100] μV were excluded. Finally, around 26 trials were reserved for each subject.

Data analysis

Reaction times

To get the reaction times of the control group, the time of each trial from audio cue to motor onset was calculated. Through this distribution, the motor onset time of the control group was estimated.

Event-related potential analysis

Usually, RPs are obtained with respect to motor onset (Russo et al. 2017). However, since the patients did not show obvious movement, it was difficult to identify their motor onset. In this study, the RPs were averaged with respect to the audio cue. Hence, the RPs obtained in this study are different from those in related literature. However, the results still showed slow rising waves and similar spatial distribution. All the cleaned trials of each subject were averaged, and the baseline window was set from − 0.2 s to 0 s before the audio cue. To observe the spatial characteristics of RP, scalp maps were plotted.

Event-related desynchronization

Event-related spectral perturbation (ERSP) was calculated by wavelet packet transform for ERD/ERS analysis between 1 and 40 Hz and the time range of − 2 s to 5 s. The Cz electrode's ERSP values were averaged for each group.

Construction of brain networks

Spectral coherence

Spectral coherence measures the correlation of two signals in the frequency domain (Pereda et al. 2005), and its formula is as follows:

$$Coh_{xy} = \left| \frac{P_{xy}}{p_{xx}p_{yy}} \right|$$

where P_{xy} is the cross-spectral density between two neural signals at electrodes x and y, and P_{xx} and P_{yy} are the auto-spectral densities for electrodes x and y.

Debiased weighted phase lag index

The weighted phase lag index measures angle differences based on their distance from the real axis. Its formula is as follows:

$$wPLI_{xy} = \frac{n^{-1}\sum_{t=1}^{n}\left|imag(S_{xyt})\right|\mathrm{sgn}(imag(S_{xyt}))}{n^{-1}\sum_{t=1}^{n}\left|imag(S_{xyt})\right|}$$

where $imag(S_{xyt})$ indicates the imaginary part of the cross-spectral from electrodes x and y, and sgn indicates the sign (–1 for negative values, + 1 for positive values, and 0 for values equal to zero). The dwPLI of phase relationships is an estimator of scalp-level connectivity that is more robust and partially invariant to volume conduction in comparison to other estimators (Peraza et al. 2012).

In the present study, the spectral COH and dwPLI measures were computed to estimate the functional connectivity between electrodes (Vinck et al. 2011) using the FieldTrip toolbox in MATLAB (Oostenveld et al. 2011). The COH and dwPLI networks were constructed in delta (1–4 Hz), theta (4–8 Hz), alpha (8–13 Hz), beta (13–30 Hz), and gamma (30–45 Hz) bands. For each band, 35% of the connectivity matrix was set to one, and other values were set to zero according to the functional connection strength. Then, all the trials of each subject were averaged, resulting in the averaged value of the COH and dwPLI connectivity matrices for each subject.

Brain network measures

Two network measures, degree and global efficiency (Latora and Marchiori 2001), were used to explore the properties corresponding to information processing in the human brain network. Brain-network measurement algorithms were implemented by the Brain Connectivity Toolbox (Rubinov and Sporns 2010).

Statistical analysis

For the node degree value of each channel analysis, a two-tailed t-test was performed at each channel between any two groups. To reduce the false positive rate for multiple comparisons, statistical tests were corrected with the BHFDR method (Benjamini and Hochberg 1995). When testing the significant changes of the COH and dwPLI network properties among the UWS, MCS, and control groups, ANOVA was applied. Post hoc analysis was performed between any two groups. To assess the relationships between patients' behavioral score and network properties, Pearson's correlation coefficients between CRS-R motor function scores and network properties were calculated.

Results

Event-related potential results

Figure 2a shows the movement onset distribution of all the subjects in the control group. The distribution curve reached the peak at about 1.1 s after the audio cue. Figure 2b shows the grand average ERP waveforms of the Cz channel. The control group showed a slowly rising negative potential 0.5 s to 1.3 s after the audio cue, but the waveform was influenced by the audio evoked potential. Similarly, patients in the MCS group showed an RP-like potential 1.8 s to 2.6 s after audio, which is consistent with the RP waveform reported in the relevant literature (Russo

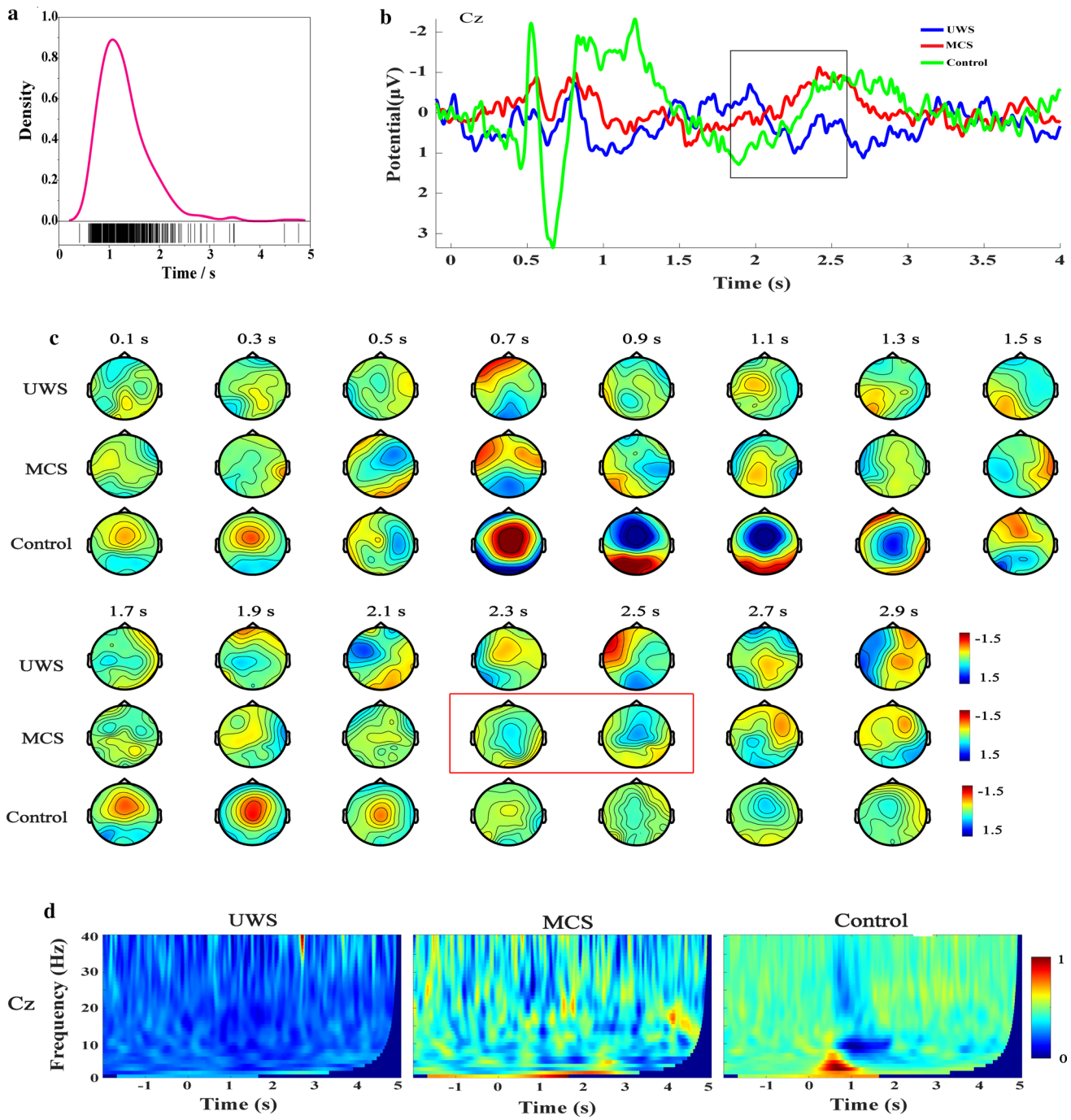

Fig. 2 The results of ERP analysis for UWS, MCS, and control groups. **a** Movement onset distribution of subjects in control group. **b** Grand average ERP waveforms of Cz channel. **c** Scalp topography sequence of ERP. **d** Time–frequency maps of Cz channel

et al. 2017; Schurger et al. 2021). However, the RP-like potential obtained in this study lasted for a shorter time. This is because the epochs were extracted based on the audio cue onset rather than the classical onset of the movement. No RP-like potential was found in the UWS group.

To verify that the RP-like potential was truly an RP and reflected the motor preparation process, the ERP's scalp topography and the time–frequency map were further analyzed. Figure 2c shows the grand average scalp topography sequence of ERP from 0 to 3 s. In the control group, the scalp topography showed a negative deflection above the frontal-parietal lobe from 0.9 s to 1.3 s. The patients in the MCS group showed the same results above the frontal-parietal lobe from 2.3 s to 2.5 s. These spatially distributed characteristics of scalp topography are also consistent with

the RP (Schmidt et al. 2016). The above phenomenon did not appear in the UWS group. Figure 2d shows the grand average time–frequency map of the Cz channel. The control group has a significant power decrease 1 s after the audio cue in the alpha and beta bands. The MCS group also had a weak low-alpha band power reduction after the audio cue. The results are consistent with the ERD phenomenon reported in the relevant literatures (Wang et al. 2020; Mohseni et al. 2020). The UWS group did not exhibit the ERD phenomenon after the audio cue. In summary, RP was observed in the MCS group but not in the UWS group.

COH networks

The scalp distributions of the COH network node degree value in the delta, theta, alpha, beta, and gamma bands are illustrated in Fig. 3a. In the theta and alpha bands, the control group had a higher node degree value in the central area of the frontal lobe. The MCS group had a higher degree of nodal value in the right area of the frontal lobe, but the UWS group did not show this phenomenon. To find the channels showing significant difference, ANOVA post hoc comparison among the three groups was performed. Comparing the MCS and UWS groups, there were significant differences in the FC3 and CP3 channels in the delta band, the FT7, F4, and FC4 channels in the theta band, and the F4, FC4, and C4 channels in the alpha band ($P < 0.05$, FDR corrected). Comparing the control and UWS groups, there were significant differences in the F8 and FT8 channels in the delta band, the FP1, F3, Fz, FCz, Cz, and Pz channels in the theta band, the FP1, Fz, FCz, Cz, and Pz channels in the alpha band, and the Pz channel in the beta band ($P < 0.05$, FDR corrected). Comparing the MCS and control groups, there were significant differences in the T3, C3, F4, and FT8 channels in the delta band, the FT8, Fz, FCz, Cz, and Pz channels in the theta band, the Fz, FCz, Cz, and FT8 channels in the alpha band, the CP3 and FT8 channels in the beta band, and the FT8 channel in the gamma band ($P < 0.05$, FDR corrected). The results demonstrated that the node degree characteristics of the three groups had significant differences in the theta and alpha bands, and the channels were mainly distributed on the movement-related brain areas. Therefore, the node degree values of seven electrodes (Fz, F4, FCz, FC4, Cz, C4, and Pz) were averaged for further analysis.

Figure 3b and c show the box-normal curves of the average node degree values for the theta and alpha bands. The node degree values of the theta and alpha bands in the control group were the highest, followed by the MCS group and then the UWS group. There were significant differences among the three groups ($P < 0.05$, FDR corrected).

dwPLI networks

Figure 4a shows the grand average connection matrix of the dwPLI networks in the delta, theta, alpha, beta, and gamma bands. In the theta band, the connections of the MCS and control groups were higher than that of the UWS group, but not significantly. In the alpha band, the connection strength of the control group was highest. The UWS group had the lowest connection strength. In the delta, beta, and alpha bands, the three groups did not show differences. Therefore, the functional connection matrix of the first 14 channels was selected for further analysis. The positions of the 14 selected channels are shown in Fig. 4d. Figure 4b shows the global efficiency value in the theta band. The control group had the highest global efficiency value, and the UWS group had the lowest global efficiency value. There was a significant difference between the UWS and MCS groups as well as between the UWS and control groups ($P < 0.01$, FDR corrected). Figure 4c shows the global efficiency value in the alpha band. Similarly, the global efficiency value of the control group was the highest, and that of the UWS group was the lowest. There was a significant difference between the UWS and control groups ($P < 0.01$, FDR corrected).

Correlation of network properties and motor function scores

Figure 5a and b show the Pearson's correlation results between the CRS-R motor function score and COH network degree in the theta and alpha bands. The COH network degrees of these two bands had significant linear correlations with the motor function scores (Degree-Theta: $r = 0.45$, $P < 0.0001$; Degree-Alpha: $r = 0.49$, $P < 0.0001$). Figure 5c and d show the Pearson's correlation results between the CRS-R motor function score and dwPLI network global efficiency in the theta and alpha bands. Similarly, the dwPLI network global efficiencies of these two bands had linear correlations with the motor function scores (GE-Theta: $r = 0.21$, $P = 0.08$; GE-Alpha: $r = 0.28$, $P < 0.05$).

Discussion

The aim of this study was to explore biomarkers that can be used to evaluate the residual motor function of DOC patients. Therefore, the ERP, COH, and dwPLI networks of the motor preparation process were analyzed. The results demonstrated that, compared with the UWS group, (1) the MCS group exhibited obvious RP during the motor preparation process; (2) the node degree properties of the

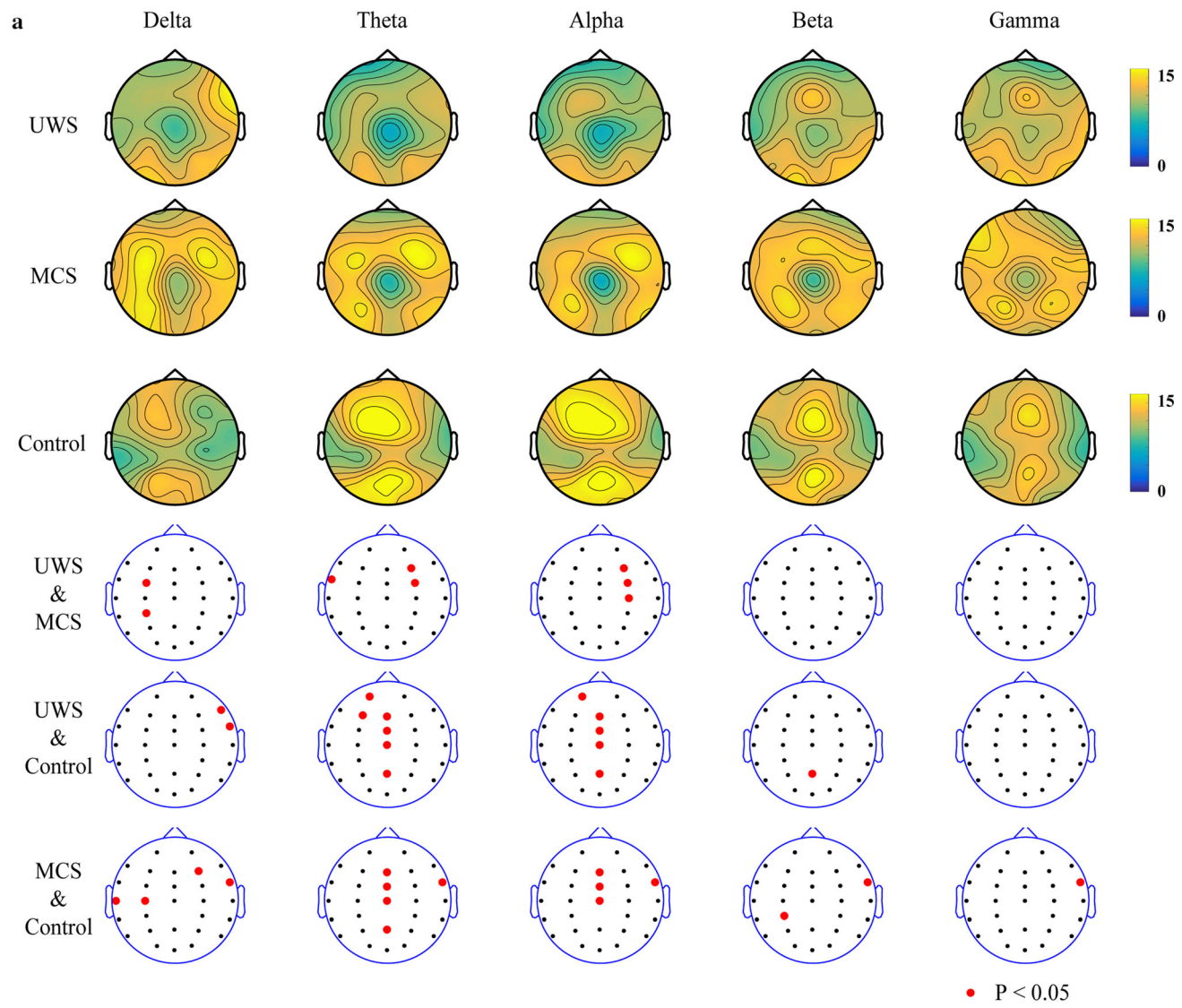
a
Delta
Theta
Alpha
Beta
Gamma
UWS
MCS
Control
UWS & MCS
UWS & Control
MCS & Control
15
0
P < 0.05

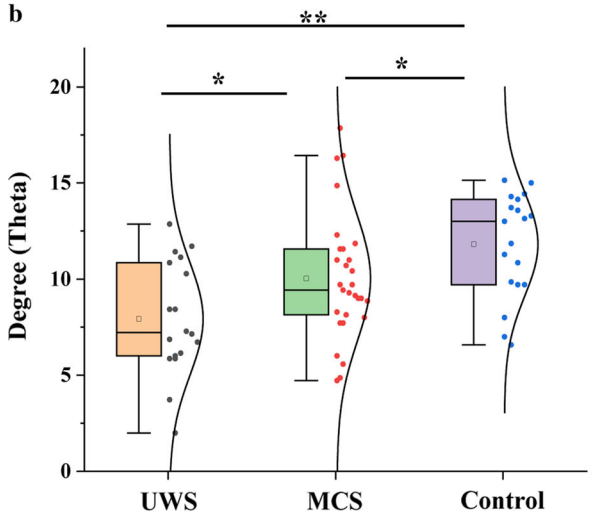
b
**
*
*
Degree (Theta)
20
15
10
5
0
UWS
MCS
Control

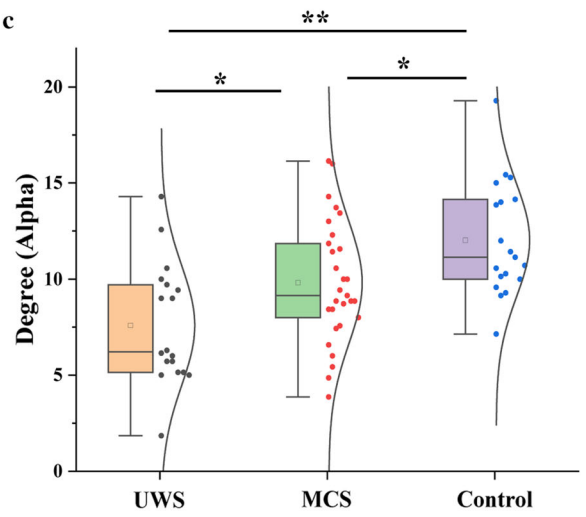
c
**
*
*
Degree (Alpha)
20
15
10
5
0
UWS
MCS
Control

◀**Fig. 3** Node degree characteristics of COH networks in delta, theta, alpha, beta, and gamma bands. **a** Scalp distribution of node degree value. **b**, **c** Box-normal curves of the average node degree values (Fz, F4, FCz, FC4, Cz, C4, and Pz) for (**b**) theta and (**c**) alpha bands (*$P < 0.05$, **$P < 0.01$, FDR corrected)

theta and alpha band COH network significantly increased in the MCS group; (3) the global efficiency properties of the dwPLI network in the theta band significantly increased in the MCS group; and (4) there was a strong linear cor-

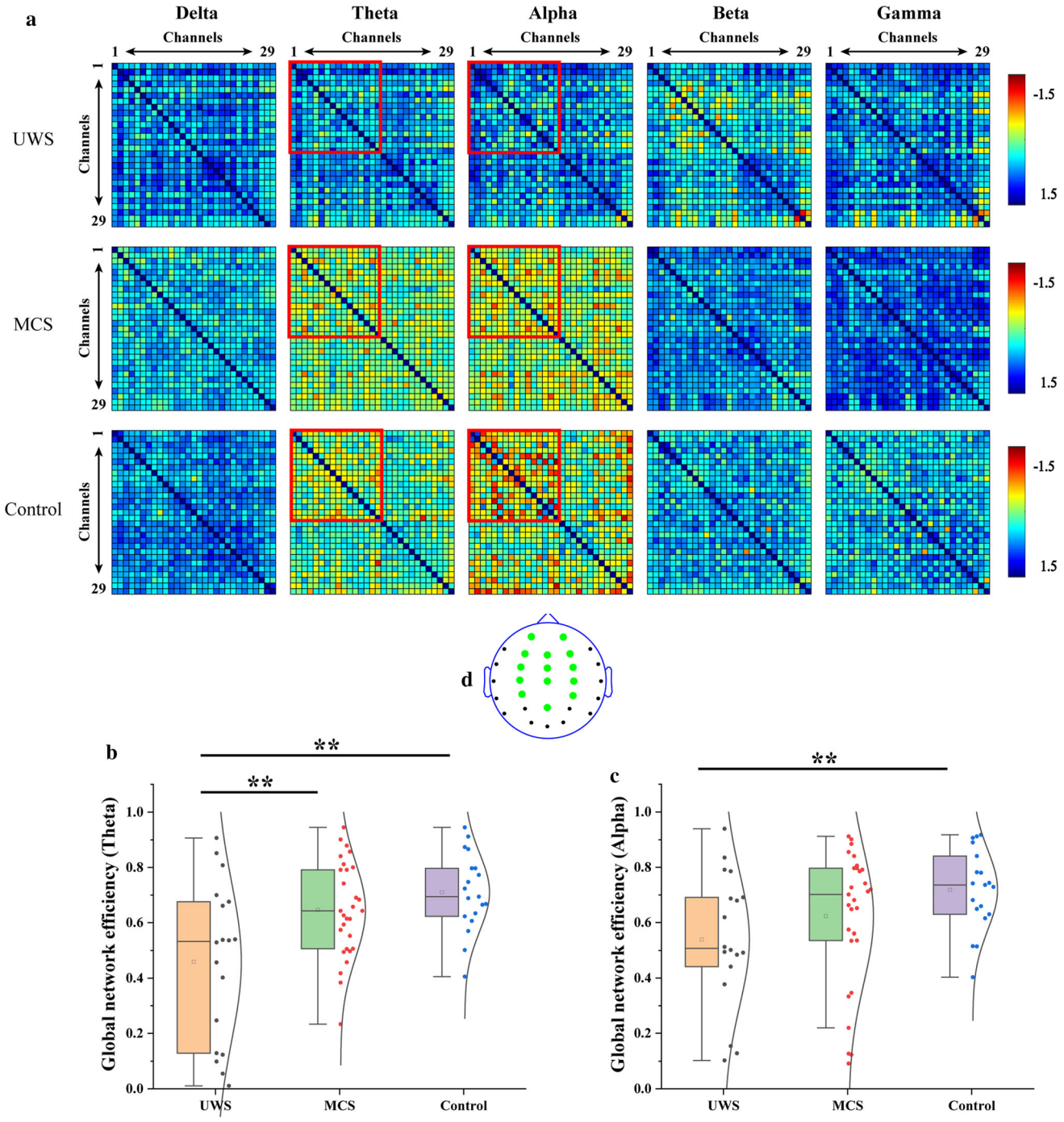

Fig. 4 Global efficiency characteristics of dwPLI networks in the delta, theta, alpha, beta, and gamma bands. **a** The grand average connection matrix of the dwPLI network. (**b**, **c**) The global network efficiency of 1–14 channels in (**b**) theta and (**c**) alpha bands (**$P < 0.01$, FDR corrected). **d** The positions of 14 selected channels (green dot). (Color figure online)

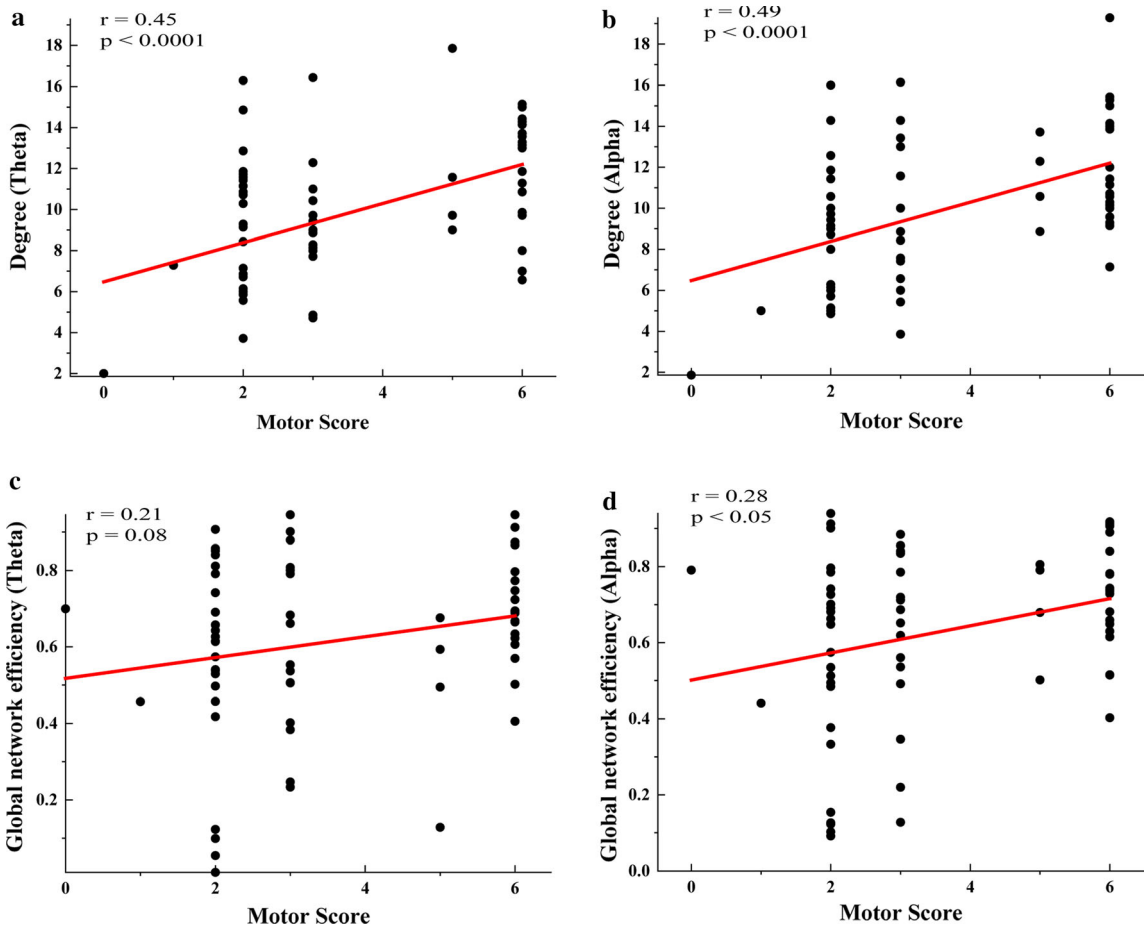

Fig. 5 Correlations between network properties and motor function score. **a**, **b** Pearson's correlation between motor function score and degree in (**a**) theta and (**b**) alpha bands. **c**, **d** Pearson's correlation between motor function score and degree in (**c**) theta and (**d**) alpha bands. The subjects with a 6-point motor score are healthy controls

relation between the above network properties and the CRS-R motor function score.

Currently, researchers generally deem that the RP reflects the motor planning and preparation process (Klimkeit et al. 2005; Liu et al. 2017). Even if there is no follow-up motor execution, the RP can still be obtained through motor imaging (Wang et al. 2020). In the grand average ERP results, the MCS group showed obvious RP. The result indicated that some patients in the MCS group could understand the audio cue and try to complete the required motor tasks. However, owing to the damage of the brain's neural network, no motor action occurred. This result confirmed the separation of cognitive and motor functions in some DOC patients reported previously (Cruse et al. 2011; Pan et al. 2020). Compared with the MMN, P1, N1, and P300 components, which have been used in consciousness assessment (Bai et al. 2020), RP relies on higher level consciousness and cognitive functions, so it could provide more valuable information for consciousness assessment. The onset of each epoch in this study was not calculated according to the traditional hand movement, and each participant completed few trials, so the individual RP's waveform was unstable, which made it difficult to provide high-quality consciousness assessment information.

The power of the EEG signal was adopted in constructing the COH network because the power-based connectivity could represent the number of neurons or spatial extent of the neural population (Pereda et al. 2005). Therefore, the COH network could reflect the size of the neural population participating in the motor preparation process. Patients in the MCS group had a higher degree of nodal value in the right-frontal area. The results were consistent with the enhancement of the COH brain network connection in the motor-related brain area during the motor preparation process reported by our previous study (Zhang et al. 2020). The statistical results showed that the nodes with significant differences between the three groups were mainly distributed in the motor-related brain areas. As expected, the results indicated that the number of neurons involved in the motor preparation process was larger in the MCS group than in the UWS group. In other words, the

patients in the MCS group retained a more complete motor function network. The results also proved the rationality of using the COH network properties to assess the patient's state of consciousness.

Only the phase of the EEG signal was applied in constructing the dwPLI network, and the phase-based connectivity likely represented the information interaction between different neural populations (Vinck et al. 2011). The dwPLI network could reflect the information communication ability of the brain areas during the motor preparation process. Accordingly, the dwPLI network connection strength of patients in the MCS group was significantly stronger than that in the UWS group. The connection strengths with obvious differences were mainly distributed in the frontal and parietal areas of the scalp (the first 14 electrodes). The results indicated that, in the MCS group, the information interaction capability among neural populations was stronger and the remaining network connections between brain areas were better preserved. In this study, the COH and dwPLI networks could evaluate the patient's residual motor function from two perspectives: the number of residual neurons in motor-related brain regions and the connection strength between neural populations.

There was a strong correlation between the network properties and the CRS-R motor function score in this study. Similarly, recent studies based on resting state EEG showed that DOC patients with a better state of consciousness tended to show stronger functional connectivity. The results of the present study indicated that the COH and dwPLI network properties of the motor preparation process could be used for the assessment of consciousness level. The research is significant due to the lack of task-state characteristics in consciousness assessment, and it will help us improve the accuracy of consciousness level assessment. This study was mainly based on the scalp EEG signal, which offers insufficient spatial resolution when characterizing inter-brain information exchange. In future studies, fMRI and EEG technology can be integrated to ensure the time accuracy of the signal and improve the spatial resolution of the brain areas.

This study calculated the brain network characteristics during motor preparation and analyzed the correlation with the motor function score. Our results confirmed that these brain network properties could be markers of residual motor function of DOC patients.

Supplementary Information The online version contains supplementary material available at https://doi.org/10.1007/s11571-021-09741-7.

Acknowledgements This research was supported by the Technology Project of Henan Province (No. 202102310210); the Key Project of Discipline Construction of Zhengzhou University (No. XKZDQY201905); the Chinese National Natural Science Foundation (No. 82001112); the Medical science and Technology research project of Henan Province (No. LHGJ20190409); the National Key R&D Program of China (2020YFC2006100) and the National Natural Science Foundation of China (No. 61803342). We thank LetPub (www.letpub.com) for its linguistic assistance during the preparation of this manuscript.

Data availability The raw EEG data can be acquired by contacting the corresponding author.

Declarations

Conflict of interest The authors declare that they have no conflict of interest. Written, informed consent was obtained from the patients for the publication of any potentially identifiable data included in this article.

References

Bai Y, Xia X, Li X (2017a) A review of resting-state electroencephalography analysis in disorders of consciousness. Front Neurol 8:471

Bai Y, Xia X, Kang J et al (2017b) TDCS modulates cortical excitability in patients with disorders of consciousness. Neuroimage Clin 15:702–709

Bai Y, Lin Y, Ziemann U (2020) Managing disorders of consciousness: the role of electroencephalography. J Neurol 268(11):4033–4065

Benjamini Y, Hochberg Y (1995) Controlling the false discovery rate: a practical and powerful approach to multiple testing. J Roy Stat Soc Ser B (methodol) 57(1):289–300

Bodart O, Gosseries O, Wannez S et al (2017) Measures of metabolism and complexity in the brain of patients with disorders of consciousness. Neuroimage Clin 14:354–362

Cruse D, Chennu S, Chatelle C et al (2011) Bedside detection of awareness in the vegetative state: a cohort study. Lancet 378(9809):2088–2094

Delorme A, Makeig S (2004) Eeglab: an open source toolbox for analysis of single-trial EEG dynamics including independent component analysis. J Neurosci Methods 134(1):9–21

di Russo F, Berchicci M, Bozzacchi C et al (2017) Beyond the "Bereitschaftspotential": action preparation behind cognitive functions. Neurosci Biobehav Rev 78:57–81

Giacino JI, Ashwal S, Childs N et al (2002) The minimally conscious state: definition and diagnostic criteria - Reply. Neurology 59(9):1473–1474

Giacino JT, Kalmar K, Whyte J (2004) The JFK coma recovery scale-revised: measurement characteristics and diagnostic utility. Arch Phys Med Rehab 85(12):2020–2029

Giacino JT, Fins JJ, Laureys S et al (2014) Disorders of consciousness after acquired brain injury: the state of the science. Nat Rev Neurol 10(2):99–114

Gui P, Jiang Y, Zang D et al (2020) Assessing the depth of language processing in patients with disorders of consciousness. Nat Neurosci 23(6):761–770

Hu Y, Zhang L, Chen M et al (2017) How electroencephalogram reference influences the movement readiness potential? Front Neurosci 11:683

Jung TP, Makeig S, Westerfield M et al (2000) Removal of eye activity artifacts from visual event-related potentials in normal and clinical subjects. Clin Neurophysiol 111(10):1745–1758

Klimkeit EI, Mattingley JB, Sheppard DM et al (2005) Motor preparation, motor execution, attention, and executive functions in attention deficit/hyperactivity disorder (ADHD). Child Neuropsychol 11(2):153–173

Kornhuber HH, Deecke L (1965) Changes in the brain potential in voluntary movements and passive movements in man: readiness potential and reafferent potentials. Pflugers Arch Gesamte Physiol Menschen Tiere 284(6):1–17

Latora V, Marchiori M (2001) Efficient behavior of small-world networks. Phys Rev Lett 87(19):198701

Laureys S, Celesia GG, Cohadon F et al (2010) Unresponsive wakefulness syndrome: a new name for the vegetative state or apallic syndrome. Bmc Med. https://doi.org/10.1186/1741-7015-8-68

Li R, Song WQ, Du JB et al (2015) Connecting the P300 to the diagnosis and prognosis of unconscious patients. Neural Regen Res 10(3):473–480

Liu TJ, Li FL, Jiang Y et al (2017) cortical dynamic causality network for auditory-motor tasks. IEEE Trans Neural Sys Rehabil Eng 25(8):1092–1099

Malagurski B, Peran P, Sarton B et al (2019) Topological disintegration of resting state functional connectomes in coma. Neuroimage 195:354–361

Mohseni M, Shalchyan V, Jochumsen M et al (2020) Upper limb complex movements decoding from pre-movement EEG signals using wavelet common spatial patterns. Comput Methods Progr Biomed 183:105076

Mouthon AL, van Hedel HJA, Meyer-Heim A et al (2016) High-density electroencephalographic recordings during sleep in children with disorders of consciousness. Neuroimage Clin 11:468–475

Naro A, Bramanti P, Leo A et al (2016) Transcranial alternating current stimulation in patients with chronic disorder of consciousness: a possible way to cut the diagnostic Gordian knot? Brain Topogr 29(4):623–644

Naro A, Bramanti A, Leo A et al (2018) Shedding new light on disorders of consciousness diagnosis: the dynamic functional connectivity. Cortex 103:316–328

Nguyen VT, Breakspear M, Cunnington R (2014) Reciprocal interactions of the SMA and cingulate cortex sustain premovement activity for voluntary actions. J Neurosci 34(49):16397–16407

Oostenveld R, Fries P, Maris E et al (2011) FieldTrip: open source software for advanced analysis of MEG, EEG, and invasive electrophysiological data. Comput Intell Neurosci 2011:156869

Pan J, Xie Q, Qin P et al (2020) Prognosis for patients with cognitive motor dissociation identified by brain-computer interface. Brain 143(4):1177–1189

Peraza LR, Aziz URA, Gary G et al (2012) Volume conduction effects in brain network inference from electroencephalographic recordings using phase lag index. J Neurosci Methods 207(2):189–199

Pereda E, Quiroga RQ, Bhattacharya J (2005) Nonlinear multivariate analysis of neurophysiological signals. Prog Neurobiol 77(1–2):1–37

Pfurtscheller G, da Silva FHL (1999) Event-related EEG/MEG synchronization and desynchronization: basic principles. Clin Neurophysiol 110(11):1842–1857

Ragazzoni A, Pirulli C, Veniero D et al (2013) Vegetative versus minimally conscious states: a study using TMS-EEG, sensory and event-related potentials. PLoS ONE 8(2):e57069

Risetti M, Formisano R, Toppi J et al (2013) On ERPs detection in disorders of consciousness rehabilitation [J]. Front Human Neurosci. https://doi.org/10.3389/fnhum.2013.00775

Rohaut B, Faugeras F, Chausson N et al (2015) Probing ERP correlates of verbal semantic processing in patients with impaired consciousness. Neuropsychologia 66:279–292

Rossi Sebastiano D, Visani E, Panzica F et al (2018) Sleep patterns associated with the severity of impairment in a large cohort of patients with chronic disorders of consciousness. Clin Neurophysiol 129(3):687–693

Rubinov M, Sporns O (2010) Complex network measures of brain connectivity: uses and interpretations. Neuroimage 52(3):1059–1069

Schiff ND, Plum F (2000) The role of arousal and "gating" systems in the neurology of impaired consciousness. J Clin Neurophysiol 17(5):438–452

Schmidt S, Jo HG, Wittmann M et al (2016) "Catching the waves" - slow cortical potentials as moderator of voluntary action. Neurosci Biobehav R 68:639–650

Schnakers C, Vanhaudenhuyse A, Giacino J et al (2009) Diagnostic accuracy of the vegetative and minimally conscious state: clinical consensus versus standardized neurobehavioral assessment. BMC Neurol. https://doi.org/10.1186/1471-2377-9-35

Schurger A, Hu P, X, et al (2021) What is the readiness potential? Trends Cognit Sci 25(7):558–570

Shibasaki H, Hallett M (2006) What is the Bereitschaftspotential? Clin Neurophysiol 117(11):2341–2356

Stefan S, Schorr B, Lopez-Rolon A et al (2018) Consciousness indexing and outcome prediction with resting-state EEG in severe disorders of consciousness. Brain Topogr 31(5):848–862

Vinck M, Oostenveld R, van Wingerden M et al (2011) An improved index of phase-synchronization for electrophysiological data in the presence of volume-conduction, noise and sample-size bias. Neuroimage 55(4):1548–1565

Wang K, Xu M, Wang Y et al (2020) Enhance decoding of pre-movement EEG patterns for brain-computer interfaces. J Neural Eng 17(1):016033

Wislowska M, Del Giudice R, Lechinger J et al (2017) Night and day variations of sleep in patients with disorders of consciousness. Sci Rep 7(1):266

Wisniewski D, Goschke T, Haynes JD (2016) Similar coding of freely chosen and externally cued intentions in a fronto-parietal network. Neuroimage 134:450–458

Yao DZ (2001) A method to standardize a reference of scalp EEG recordings to a point at infinity [J]. Physiol Meas 22(4):693–711

Zhang L, Wang P, Zhang R et al (2020) The influence of different EEG references on scalp EEG functional network analysis during hand movement tasks. Front Hum Neurosci 14:367